F_oF_1-ATPase, rotary motor and biosensor

Yao-Gen Shu,*[a] Jia-Chang Yue*[b] and Zhong-Can Ou-Yang[a]

Received 15th December 2009, Accepted 1st March 2010
DOI: 10.1039/b9nr00411d

F_oF_1-ATPase is an amazing molecular rotary motor at the nanoscale. Single molecule technologies have contributed much to the understanding of the motor. For example, fluorescence imaging and spectroscopy revealed the physical rotation of isolated F_1 and F_o, or F_oF_1 holoenzyme. Magnetic tweezers were employed to manipulate the ATP synthesis/hydrolysis in F_1, and proton translation in F_o. Here, we briefly review our recent works including a systematic kinetics study of the holoenzyme, the mechanochemical coupling mechanism, reconstituting the δ-free F_oF_1-ATPase, direct observation of F_o rotation at single molecule level and activity regulation through external links on the stator.

I. Introduction

F_oF_1-ATPase is a ubiquitous rotary motor that uses the transmembrane electrochemical potential to synthesize ATP in the plasma membrane of bacteria, chloroplasts and mitochondria. The holoenzyme is a complex of two rotary motors, F_o and F_1, which are mechanically coupled by a common central stalk ("rotor"), $c_n\varepsilon\gamma$. The membrane embedded F_o unit converts the proton motive force (p.m.f.) into mechanical rotation of the "rotor", thereby causing cyclic conformational change of $\alpha_3\beta_3$ crown ("stator") in F_1 and driving ATP synthesis. A striking characteristic of this motor is its reversibility. It may rotate in the reverse direction for ATP hydrolysis and utilize the excess energy to pump protons across the membrane.[1–6]

[a]*Institute of Theoretical Physics, CAS, Beijing, 100190, China. E-mail: shuyg@itp.ac.cn*
[b]*Institute of Biophysics, CAS, Beijing, 100101, China. E-mail: yuejc@sun5.ibp.ac.cn*

The basic hypothesis, "binding change mechanism",[7] however, had not been confirmed until direct observation of the rotation of F_1-ATPase at the single molecule level in 1997,[8] although it was partly proven by the eccentric structure of the γ subunit in 1994.[9] Single molecule technologies have contributed much to the understanding of the motor. For example, fluorescence imaging and spectroscopy revealed the physical rotation of isolated F_1[8,10–12] and F_o,[13,14] or F_1F_o holoenzyme.[15–17] Magnetic tweezers also be employed to manipulate the ATP synthesis/hydrolysis in F_1,[18,19] and proton translation in F_o.[20] Nevertheless, the fundamental relation between the rotation speed and substrate/product concentrations, transmembrane p.m.f. and damping coefficient is important in the time frame of enzymatics.[21]

II. Systematic kinetics of the holoenzyme

A few theoretical approaches have been proposed, aiming for a better understanding of the operating mechanism of this reversible motor. Some work focused on the hydrolysis or synthesis of F_1. For example, Oster *et al.* constructed a 4^3 states

Yao-Gen Shu

Y.-G. Shu was born on January 4, 1964 in Zhejiang province, China. He received his Bachelor of Electronic Engineering in July 1985 at Zhejiang University, and then worked on industrial automation till 1999. He received his Ph. D. in 2004 at the Department of Physics of Xiamen University. From 2004 to 2009, he worked with Prof. Zhong-Can Ou-Yang at the Institute of Theoretical Physics (Chinese Academy of Sciences) and Prof. Pik-Yin Lai at the National Central University (Taiwan), respectively. Currently, he is a research fellow at the Institute of Theoretical Physics. His research focuses on molecular motors, cell motion, biosensor, nanodevices, and so on.

Jia-Chang Yue

Prof. Jia-Chang Yue is the leader of the molecular motor group at the Institute of Biophysics at the Chinese Academy of Sciences. He has held positions as a visiting scholar at Tohoku University, Japan and Hong Kong Polytechnic University. Previously he researched at the Department of Engineering Physics, Tsinghua University, China. Current research interests include: the structure and function of the rotary molecular motor FoF1-ATPase, and developing biosensors based on FoF1-ATPase.

model for the couplings among three catalytic sites and provided a physical view of the dynamics.[22–24] However, this model is too sophisticated to be investigated analytically. Some other models studied the mechanism of torque generation of F_o with a turbine or all-atom model.[25–27] The kinetics of the motor have also been investigated by Pänke *et al.* with simulations or storage of elastic energy model.[28,29] Here, we focus on an analytical investigation of the systematic kinetics of the holoenzyme, that is, the fundamental relation between the rotation speed and substrate/product concentrations, transmembrane p.m.f. and damping coefficient.[21]

It is well established that the mechanical process in F_o and the chemical reactions in F_1 are tightly coupled. Therefore, it is possible to construct a theory which can systematically describe the whole machine. From the view point of enzymatics, conventional theory generally concerned with irreversible reaction on a single substrate which can be described by Michaelis–Menten kinetics. But ATP can be reversibly synthesized and hydrolyzed in F_oF_1-ATPase, and the reaction involves several substrates/products, thus there is an need for a quantitative theory which describes the multi-substrate/product enzymatics. Furthermore, analytical results could presumably allow for a deeper insight for the working principles of the motor.

F_oF_1-ATPase, in particular, is an amazing reversible motor. ATP hydrolysis does spontaneously occur in F_1, whereas the thermodynamically unfavorable reaction, ATP synthesis, has to be driven by harnessing the transmembrane proton flow in F_o. If the motor functions as a synthase, the two substrates, ADP and P_i, are recombined into one product, ATP. The binding order of the two substrates is a characteristic attribute of the synthase. On the basis of inhibition studies, a compulsory order with binding of ADP preceding that of P_i was proposed.[30] Enzyme kinetic analysis, on the other hand, indicated a random order in their binding.[31,32]

Another challenging question is whether the main kinetic enhancement occurs upon filling the second or the third site. Based on measurements of the dependence of ATP synthesis rate on ADP concentration, Boyer and Cross proposed that rapid net synthesis of MF_1 is attained when a second catalytic site is filled.[33,34] Results from the laboratories of Senior,[35] Allison[36] and Kinosita,[11] however, provided evidence that three catalytic sites are filled when sufficient ATP is present for rapid catalysis by EcF_1 or TF_1. A crystal structure[37] also indicated that all three sites are filled, one with ATP, one with ADP and P_i and one half closed site with ADP and P_i.

Different from the bi-site scenario, the tri-site one guarantees that the synthesis and the hydrolysis follow the same reaction pathway, which corresponds to the basic scheme that is proposed by Nakamoto, Senior and Kinosita.[12,38–40] Here, we propose a tri-site filled scenario with random order of ADP and P_i binding (shown in Fig. 1) and systematically investigate the kinetics of F_oF_1-ATPase with p.m.f. The following details are taken into account:

1. The synthesis and hydrolysis follow the same reaction pathway. One ATP is consumed if the motor moves 120° counterclockwise (CCW, blue pathway). Conversely, one ATP is synthesized if it moves 120° clockwise (CW, red pathway).

2. Before each step, all three $\alpha\beta$ pairs display different conformations depicted as "open" (green), "loose" (blue) and "tight" (red). The exchange of substrates is practically restricted to the "open" conformation.

3. The binding of ATP and ADP/P_i to the "open" site is taken to be competitive while that of ADP and P_i is random.

4. CCW 120° movement of γ drives conformational changes of the three sites as "open" → "tight", "tight" → "loose" and "loose" → "open" respectively.

5. Chemical reaction, ADP + P_i ⇌ ATP + H_2O, takes place during the "tight" ⇌ "loose" conformational change, and is tightly coupled with transmembrane proton transport in F_o by the rotation of "rotor".

Five states involved in this model are denoted by E, ET, EDP, ED and EP respectively. E is a two-site filled state and it has been indicated in the crystal structure[9] that one site binds ATP and the other grips ADP and P_i. All others are three-site filled states. The structure of EDP has also been crystallized.[37] Different from the bi-site model, the present model suggests that ATP synthesis, in the presence of adequate p.m.f., requires ADP and P_i to occupy

Zhong-Can Ou-Yang

Prof. Zhong-Can Ou-Yang was born on January 25, 1946 in Fujian province, China. He received his Ph.D. in 1984 from Tsinghua University (Beijing). From 1987–1988, he worked with Prof. W. Helfrich at the Freie University (Berlin) as an Alexander von Humboldt fellow. He has been a professor at the Institute of Theoretical Physics, Chinese Academy of Sciences since 1992, and Director from 1998–2007. His research focuses on soft condensed matter physics and theoretical biophysics. He received the Achievement in Asia Award from the Overseas Chinese Physics Association in 1993 and is a member of Chinese Academy of Sciences and the Third Word Academy of Sciences.

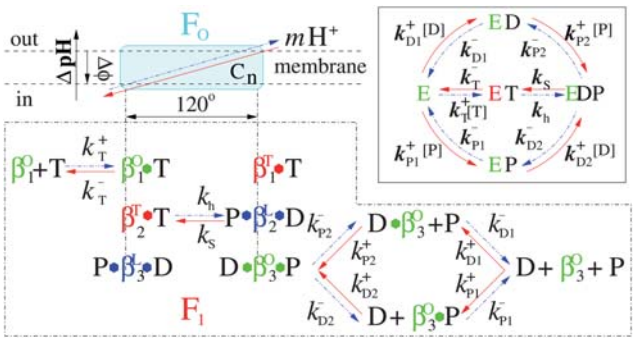

Fig. 1 The detailed coupling reaction scheme of the holoenzyme F_oF_1-ATPase. Synthesis pathway runs from right to left (red solid line), whereas hydrolysis one runs from left to right (blue dashed dots). T, D and P represent ATP, ADP and P_i respectively. The green, blue and red β subunits denote "open", "loose" and "tight" conformations (labeled by the superscripts O, L and T of β respectively) and correspond to β_E, β_{DP} and β_T in the Walker structure.[9] The inset shows the reversible reaction pathways of the enzyme F_1.[21]

the third (open) site; while for ATP hydrolysis, if the p.m.f. is low or absent, it requires that ATP occupies the same site.

The kinetics of this reversible reaction (shown in Fig. 1)[21] may be described by the equations governing the probabilities (denoted by P_E, P_{ET}, P_{EDP}, P_{ED}, and P_{EP}) of these five states

$$\left.\begin{aligned}
\dot{P}_E &= k_T^- P_{ET} + k_{D1}^- P_{ED} + k_{P1}^- P_{EP} \\
&\quad -\left(k_{D1}^+[D] + k_{P1}^+[P] + k_T^+[T]\right) P_E \\
\dot{P}_{ET} &= k_T^+[T] P_E + k_s P_{EDP} - \left(k_T^- + k_h\right) P_{ET} \\
\dot{P}_{EDP} &= k_h P_{ET} + k_{P2}^+[P] P_{ED} + k_{D2}^+[D] P_{EP} \\
&\quad -\left(k_{D2}^- + k_{P2}^- + k_s\right) P_{EDP} \\
\dot{P}_{ED} &= k_{P2}^- P_{EDP} + k_{D1}^+[D] P_E - \left(k_{D1}^- + k_{P2}^+[P]\right) P_{ED} \\
P_{EP} &= 1 - \left(P_E + P_{ET} + P_{EDP} + P_{ED}\right)
\end{aligned}\right\} \quad (1)$$

where the square bracket [ ] denotes the concentration, T, D and P represent ATP, ADP and P_i respectively, and k^+ (k^-) is the binding (unbinding) constant. The steady-state reaction rate has been derived as second order in [D] and [P], and cannot be treated in terms of a Michaelis–Menten form. However, if the bindings and unbindings of ADP and P_i are completely independent and there is no mutual interaction, *i.e.* $k_{D1}^{\pm} = k_{D2}^{\pm} \equiv k_D^{\pm}$ and $k_{P1}^{\pm} = k_{P2}^{\pm} \equiv k_P^{\pm}$, it can be put into an apparent Michaelis–Menten equation. In addition, clamped ΔpH experiment[41] has shown that binding and unbinding of a substrate (at cosubstrate saturation) are rapid processes as compared to the synthesis/hydrolysis step (mechanical rotation), which means that $k_{s/h} \ll k_L \equiv k_P^+[P] + k_D^+[D] + k_P^- + k_D^-$. Within the framework of steady-state conditions for eqn (1), the clockwise revolution rate of the motor at steady state is given by $\frac{1}{3}(k_s P_{EDP} - k_h P_{ET})$ and is computed to be

$$r_c = \frac{\frac{1}{3} v_M^s v_M^h \left\{[D][P] - \frac{[T]}{K_e}\right\}}{\left(K_M^P[D] + K_M^D[P] + [D][P]\right) v_M^h + \frac{K_M^T + \sigma[T]}{K_e} v_M^s} \quad (2)$$

the definition and meaning of various quantities in the above equation are given below:

v_M^s and v_M^h are the saturated rates of synthesis and hydrolysis and are given by

$$\begin{aligned}
v_M^s &\equiv \frac{v_{max}^s k_s}{k_s + k_h + v_{max}^s (1 - k_s/k_L)} \\
&\approx \frac{v_{max}^s k_s}{k_s + v_{max}^s + k_h},
\end{aligned} \quad (3)$$

$$\begin{aligned}
v_M^h &\equiv \frac{v_{max}^h k_h}{k_h + v_{max}^h [1 - (k_h - k_s)/k_L]} \\
&\approx \frac{v_{max}^h k_h}{k_h + v_{max}^h}
\end{aligned} \quad (4)$$

respectively, where the maximum rates are $v_{max}^s \equiv k_T^-$ and $v_{max}^h \equiv k_P^- k_D^- / (k_P^- + k_D^-)$.

The corresponding Michaelis constants are given by

$$\begin{aligned}
K_M^T &\equiv v_M^h \left[\frac{1}{k_T^-} + \frac{1}{k_h}\left(1 + \frac{k_s}{k_L}\right)\right] K_d^T \\
&\approx \left[1 - v_M^h \left(\frac{1}{v_{max}^h} - \frac{1}{k_T^-}\right)\right] K_d^T,
\end{aligned} \quad (5)$$

$$\begin{aligned}
K_M^P &\equiv v_M^s \left[\frac{1}{k_P^-} + \frac{1}{k_s}\left(1 + \frac{k_h}{k_T^-}\right)\right] K_d^P \\
&\approx \left[1 - v_M^s \left(\frac{1}{v_{max}^s} - \frac{1}{k_P^-}\right)\right] K_d^P,
\end{aligned} \quad (6)$$

$$\begin{aligned}
K_M^D &\equiv v_M^s \left[\frac{1}{k_D^-} + \frac{1}{k_s}\left(1 + \frac{k_h}{k_T^-}\right)\right] K_d^D \\
&\approx \left[1 - v_M^s \left(\frac{1}{v_{max}^s} - \frac{1}{k_D^-}\right)\right] K_d^D.
\end{aligned} \quad (7)$$

The equilibrium constant is given by $K_e \equiv K_e^b \exp\left(-\frac{\Delta G}{k_B T}\right)$, where $K_e^b \equiv K_d^T/(K_d^D K_d^P)$ and the dissociations constant are $K_d^l = k_l^-/k_l^+$ with the subscript $l = T, D, P$ respectively. The equilibrium constant varies exponentially with p.m.f.

The inhibitions between substrates and products are complicated because ATP or ADP/P_i binds competitively to the same "open" site no matter which motor functions as the synthase or hydrolase. For convenience, we express the inhibitions in an uncompetitive hydrolysis form with the parameter: $\sigma \equiv 1 + [P]/K_I^{TP} + [D]/K_I^{TD} + [D][P]/K_I^{TDP}$, where $K_I^{TP} \equiv K_d^P \chi k_D^-/k_P^-$, $K_I^{TD} \equiv K_d^D \chi k_P^-/k_D^-$, $K_I^{TDP} \equiv K_d^D K_d^P \chi / \left[1 + \exp\left(\frac{\Delta G}{k_B T}\right)\right]$, and $\chi = \exp\left(\frac{\Delta G}{k_B T}\right) k_L / v_M^h$.

Eqn (2) implies that the motor is a synthase if $r_c > 0$, a hydrolase if $r_c < 0$, and at equilibrium if $r_c = 0$. However, the relation between the rotation speed, p.m.f. and damping coefficient is still unclear. Now we use a stochastic mechanochemical coupling model to set the relation between k_h/k_s, ΔpH and the damping coefficient of the "rotor".

III. Stochastic mechanochemical coupling model

The ensemble average behavior of F_oF_1-ATPase can be described phenomenologically by standard chemical kinetics if the reaction rates and mechanical rotation rate are related and their dependence on proton translocation is known. On the microscopic scale, F_oF_1-ATPase is more naturally described as a small mechanical device driven by a series of cyclic conformational states including rapid chemical events, such as binding and unbinding of substrates/products, and incessant, fast, thermal fluctuations which is essential to the molecular mechanism.[42–44] It is at this level of microscopic fluctuations that the mechanical reversible rotation speed and chemical quantities such as concentrations of substrates/products and p.m.f. can be most naturally connected.

It is rather well-established that different phenomena, such as the reversible chemical transition ET ⇌ EDP, the cyclic conformational changes of $\alpha_3\beta_3$ crown, the couplings/communications among the three catalytic sites, and the stochastic $2\pi/3$ rotation of the "rotor", originate from the same process and occur simultaneously. In our model, E is the substrate "waiting" state, ED and EP are also substrate "waiting" states if the motor functions as a synthase. In these states, the barrier is too high for

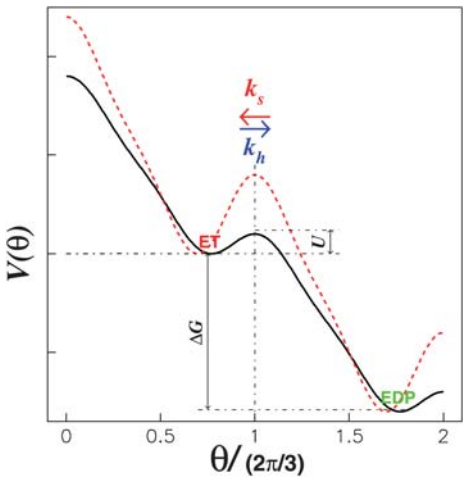

Fig. 2 Model energy landscape with a periodic tilt, $\Delta G > 0$. The drop in the barrier from the red dotted curve to the black solid curve takes place once the corresponding substrate binds to the substrate "waiting" site.[21]

the chemical transition ET $\rightleftharpoons$ EDP in β_2 to take place (dashed curve in Fig. 2). According to the binding change mechanism,[7,45] catalysis at one of the three sites is strongly promoted by additional substrate binding. For the hydrolysis pathway, ATP binding to the nucleotide-free site (β_1) opens the gate by reducing the barrier as shown in Fig. 2(solid curve), which allows another ATP in β_2 to be hydrolyzed. The free energy change of this step is given by:

$$\Delta G = \Delta G_0 - m\Delta\tilde{\mu}_{H^+} \quad (8)$$

where $\Delta G_0 \approx 20k_BT$[42], ΔG is merely related to the ATP hydrolysis reaction, and is independent of entropic and enthalpic contributions. m is the H^+/ATP ratio of proton transport-coupled ATP synthesis and hydrolysis, an important parameter for the energy balance of all cells. A straightforward interpretation of rotational catalysis predicts that m coincides with the ratio of the c-subunits to β-subunits, implying that $m = n/3$, while n ranges from 10 to 15 for different species.[46–51] The transmembrane electrochemical energy, $\Delta\tilde{\mu}^+_H$, is usually expressed in terms of the transmembrane pH difference, $\Delta pH \equiv pH_{in} - pH_{out}$, and the transmembrane electric potential, $\Delta\phi \equiv \phi_{out} - \phi_{in}$, as

$$\Delta\tilde{\mu}_{H^+} = 2.3k_BT\Delta pH + e\Delta\phi \quad (9)$$

where k_B, T and e are Boltzmann constant, absolute temperature and elementary charge respectively. At room temperature, $2.3k_BT/e \approx 59$ mV. The p.m.f. $\Delta P \equiv \Delta\tilde{\mu}_{H^+}/e = \Delta\phi + 59\Delta pH$. Eqn (9) shows that ΔpH and $\Delta\phi$ are energetically equivalent, which is an essential feature of chemiosmotic theory.[52] Experimental results on steady-state synthesis rates obtained with reconstituted ATP synthase from both spinach chloroplasts[53,54] and chromatophores of *R. capsulatus*[55] also indicated this feature.

Here, we introduce a two-dimensional energy landscape, $V(x_1, x_2)$, with chemical and position variables. The kinetics of the enzyme may then be investigated by a random walk on the energy surface. As required for cyclic chemical turnovers and mechanical rotations, the surface is periodic along the chemical and position axes except for a uniform tilt of ΔG. In the tight mechanochemical coupling step, ET $\rightleftharpoons$ EDP, however, the two-dimensional $V(x_1, x_2)$ may be reduced to an one-dimensional $V(\theta)$, where θ represents the relative position between the "rotor" and the "stator". The energy difference, ΔG, is periodically coupled into $V(\theta)$ completely due to the tight coupling between the γ rotation and $\alpha_3\beta_3$ crown conformational changes. The stochastic theory, thereby, makes it possible to obtain the rates of hydrolysis and synthesis as a function of p.m.f. since ΔG is included in $V(\theta)$.

At steady state, all quantities about the stochastic rotation of the "rotor", including the probability density of the "rotor" at an angle θ, $\rho(\theta)$, and the associated probability current, J, are constant in time, namely

$$J = -\frac{1}{D}\left(\frac{d\rho}{d\theta} + \frac{1}{k_BT}\frac{dV}{d\theta}\rho\right) \quad (10)$$

where the diffusion constant $D = k_BT/\xi_r$, in accordance with the Einstein relation between D and ξ_r. ξ_r is the rotational damping coefficient of "rotor" assembly. We solved for $\rho(\theta)$ with constant J, then set the probabilities of biochemical states ET and EDP to be $P_{ET} = \int_0^{\frac{2\pi}{3}}\rho(\theta)d\theta$ and $P_{EDP} = \int_{\frac{2\pi}{3}}^{\frac{4\pi}{3}}\rho(\theta)d\theta$ respectively. Finally, J is derived and compared with the form expected for a first-order chemical reaction at steady state, $k_hP_{ET} - k_sP_{EDP}$. The desired expressions for the rates of hydrolysis and synthesis as a function of ΔG can therefore be obtained:[56–60]

$$k_h = \frac{1}{D}\frac{\Pi_{EDP0}}{\Pi_{ET0}\Pi_{EDP} - \Pi_{EDP0}\Pi_{ET}} \quad (11)$$

$$k_s = \frac{1}{D}\frac{\Pi_{ET0}}{\Pi_{ET0}\Pi_{EDP} - \Pi_{EDP0}\Pi_{ET}} \quad (12)$$

where

$$\Pi_{ET0} = \exp\left(\frac{V(0)}{k_BT}\right)\int_0^{\frac{\pi}{3}}\exp\left(-\frac{V(\theta)}{k_BT}\right)d\theta$$

$$\Pi_{EDP0} = \exp\left(\frac{V(0)}{k_BT}\right)\int_{\frac{\pi}{3}}^{\frac{2\pi}{3}}\exp\left(-\frac{V(\theta)}{k_BT}\right)d\theta$$

$$\Pi_{ET} = \int_0^{\frac{\pi}{3}}\exp\left(-\frac{V(\theta)}{k_BT}\right)\Xi(\theta)d\theta$$

$$\Pi_{EDP} = \int_{\frac{\pi}{3}}^{\frac{2\pi}{3}}\exp\left(-\frac{V(\theta)}{k_BT}\right)\Xi(\theta)d\theta$$

and

$$\Xi(\theta) = \int_0^{\theta}\exp\left(\frac{V(\theta')}{k_BT}\right)d\theta'$$

For a potential with two wells separated by a barrier, as in Fig. 2, the rate constants are most sensitive to the distances from the well bottoms to the barrier top, the size of each well, the barrier height (U), and the energy difference between wells (ΔG). Once these parameters are specified, the detailed shape of the potential has relatively little effect.

At equilibrium the net probability current, J, must be zero, and

$$\frac{P_{EDP}}{P_{ET}} = \frac{k_h}{k_s} = \frac{\Pi_{EDP0}}{\Pi_{ET0}} = \frac{\int_{\frac{\pi}{3}}^{\frac{2\pi}{3}} \exp\left(-\frac{V(\theta)}{k_B T}\right) d\theta}{\int_{0}^{\frac{\pi}{3}} \exp\left(-\frac{V(\theta)}{k_B T}\right) d\theta} = \exp\left(\frac{\Delta G}{k_B T}\right) \quad (13)$$

because of $V(\theta + \pi/3) = V(\theta) - \Delta G$. Eqn (13) is the simple and familiar Arrhenius form, though the ΔG no longer has the same simple physical interpretation of free energy. ΔG is merely related to the ATP hydrolysis reaction, transmembrane ΔpH and $\Delta\phi$, and is independent of entropic and enthalpic contributions of substrates and products.

In order to calculate the rates of hydrolysis and synthesis that are tightly coupled to the diffusive rotation of the "rotor", the one-dimensional energy landscape is phenomenologically constructed as (see Fig. 2):

$$V(\theta) = V_0\{\sin[3(\theta+\theta_0)] + \lambda \sin[6(\theta+\theta_0)]\} - \Delta G \frac{3\theta}{2\pi} \quad (14)$$

where $\lambda = \Delta G/(4\Delta G_0)$, V_0 and θ_0 depend on the barrier U and free energy ΔG as follows:

$$\left.\frac{\partial V}{\partial \theta}\right|_{\theta=0} = 0$$

$$U = \left\{ \begin{array}{ll} V\left(\frac{2\pi}{3}\right) - V\left(\frac{2\pi}{3} - 2\theta_0\right) & \text{if } \Delta G \geq 0 \\ V\left(\frac{2\pi}{3}\right) - V\left(\frac{4\pi}{3} - 2\theta_0\right) & \text{if } \Delta G < 0 \end{array} \right\}$$

This asymmetric ratchet potential can be used to describe simultaneously the chemical transition between the two metastable states, ET and EDP, and the stochastic rotation of the "rotor" because the chemical transition ET $\rightleftharpoons$ EDP is tightly coupled to the $2\pi/3$ step rotation. The potential is constructed so that the barrier position can shift with varying ΔG. Under the conditions favoring ATP hydrolysis, that is, the p.m.f. is so low that $\Delta G > 0$, the barrier position approaches the state ET. On the other hand, under conditions favoring ATP synthesis, the barrier position is close to the state EDP. If $\Delta G = 0$, the ratchet potential will become symmetric. Such a construction is phenomenologically reasonable for the reversible motor.

Eqn (3), (6) and (7) can be directly used to quantitatively interpret the ensemble synthesis experiment of the holoenzyme[28] as shown in Fig. 3. For an isolated TF_1 with an attached long actin filament on the "rotor",[10] the hydrolysis step is the rate-limiting step because of the large damping of the long filament. Thus the hydrolysis kinetics can be easily analyzed by our model. Here, $k_s \approx 0$, and $\sigma \approx 1$ due to $v_M^h \approx k_h \ll k_L$. Eqn (2) may be simplified into a normal Michaelis form:

$$r_{cc} \approx \frac{1}{3} \frac{k_h[T]}{K'^{T}_{M} + [T]} \quad (15)$$

where r_{cc} is the CCW rotational rate of the motor, and the apparent Michaelis constant $K'^{T}_{M} \approx K^{T}_{d}\{1 + [P]/K^{P}_{d} + [D]/K^{D}_{d} + [P][D]/(K^{P}_{d}K^{D}_{d})\}$. Thus, K'^{T}_{M} is almost independent of the length of the actin filament. The CCW rotational rate of the motor can be directly related to the actin filament length L through the damping coefficient: $\xi_r = (\pi/3)\eta L^3/[\ln(L/2r) - 0.447]$,[61] where r is the radius of the attached filament and η is the medium viscosity. Then one obtains

$$\log(r_{cc}) \approx -3\log(L) + \log[\ln(L/2r)\text{-}0.447] - \log\left(1 + K'^{T}_{M}/[T]\right) + \log[F(U)] \quad (16)$$

where $F(U) = [k_B T/(\pi\eta)][\Pi_{EDP0}/(\Pi_{ET0}\Pi_{EDP} - \Pi_{EDP0}\Pi_{ET})]$. The single-molecule experimental results of r_{cc} as a function of L at different [T][10] can be fitted from eqn (16). These results are shown in Fig. 4. The parameter $F(U)$ may be used to estimate the scale of the reduced barrier (black solid curve in Fig. 2) which gives $U \approx 2k_B T$. In contrast to Oster's 64 states model,[24] the analytical results from our model can directly fit the single-molecule experimental data with just two parameters, one being the hydrolysis Michaelis constant and the other is the barrier of the mechanochemical coupling potential.

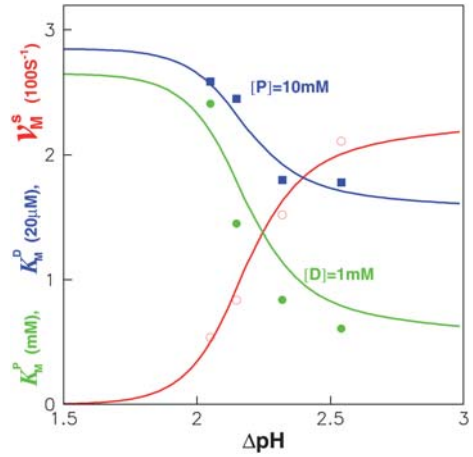

Fig. 3 Experimental data[28] of v_M^s, K_M^D and K_M^P *versus* ΔpH fitted by our model with $v_{max}^s = 250\ s^{-1} (\ll k_{-P})$, $K_d^D = 57\mu M$, $K_d^P = 2.65$ mM and $k_{-D} = 500\ s^{-1}$. Here, $\Delta\phi = 0$ mV, $m = 4$,[62,63] and $U = 3k_B T$. Damping coefficient $\xi_r = 6\pi\eta_b h r^2$, is mainly contributed by the friction between c-ring and membrane, where $h = 10$ nm, is the "rotor" height, and $r = 5$ nm, is its radius.[64] The bilayer viscosity is taken to be $\eta_b = 10^{-7}$ pN s nm^{-2}.[21,25]

IV. Direct observation of the light-driven rotation of F_o motor

Single molecule experiments had indicated the rotation of the F_1 motor with a fluorescent filament attached the γ subunit.[8,10] The relative rotation between the stator and rotor of the holoenzyme also had been detected by the FRET between the ε and b subunits.[16] F_o is an ion-driven rotary motor. Its "rotor" is the proton channels c_n and is connected the γ subunit by the ε subunit. Its "stator" consists of the a and b_2 subunits and is fixed to the $\alpha_3\beta_3$ crown of F_1 by the δ subunit. Once the δ subunit is deleted, the two "stators" are no longer coupled, and the $\alpha_3\beta_3$ crown will accompany the "rotor" on rotation. This is named δ-free F_oF_1-ATPase. We had developed a method to reconstitute the hybrid δ-free F_oF_1-ATPase and bacteriorhodopsins (BRs) into a liposome.[13,65] BR converts light energy into transmembrane p.m.f., while the liposome functions as a battery to drive the motor. Employing a fluorescent actin filament attached

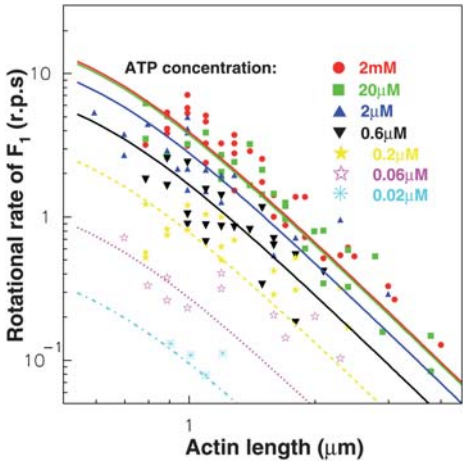

Fig. 4 The CCW rotational rate of an isolated TF_1 *versus* L at different ATP concentrations. Symbols come from experiment[10] while curves are fitted by our model with parameters $K'^{M}_{T} = 0.8\ \mu M$ and $U = 2k_BT$. Here $\xi_r = (\pi/3)\eta L^3/[\ln(L/2r) - 0.447]$[61] with the radius of filament $r = 5$ nm and the medium viscosity $\eta = 10^{-9}$ pN s nm^{-2}.[21]

to the β subunit, we have observed the light-driven rotation of δ-free F_oF_1-ATPase motor directly at the single molecule level.[13]

The procedure of δ subunit deletion of F_oF_1-ATPase is briefly shown in Fig. 5. The proteoliposome containing F_oF_1-ATPase and BR was incubated with 2 M LiCl, 0.1 mM tricine-NaOH, 10 mM $MgCl_2$, and 1 mM ATP for 20 min at 4 °C. Then the proteoliposome was washed and isolated by centrifuging. Because some α and β subunits may also be removed during δ deletion, the LiCl-treated proteoliposome needs incubation with purified $\alpha_3\beta_3\gamma$(or β) subunits at 4 °C for 60 min (for each divided subunit of F_1 with buffer 0.1 mM tricine-NaOH, 10 mM $MgCl_2$, 50 mM KCl, 0.5 mM NaCl, and 1 mM ATP), and then is cultured at 37 °C for 60 min (for reconstituting the δ-free F_oF_1-ATPase). The proteoliposome needs to be isolated to obtain the reconstituted δ-free F_oF_1-ATPase.[66–68]

To visualize the rotation of F_o in proteoliposome, a fluorescently labeled actin filament was attached to β subunits through His-tag, and the proteoliposome was immobilized onto the glass surface through the biotin–streptavidin–biotin complexes (Fig. 6A). The sample was exposed under the cooled light source with a 570 nm filter for 30 min to initiate the rotation of the F_o motor. Before illumination, the buffer containing 2 mM NaN_3 and 2 mM ADP was infused into the chamber. The clockwise rotation of the actin filament was traced directly by an Olympus IX71 fluorescent microscope equipped with an ICCD camera (Roper Scientific, Pentamax EEV 512 × 512 FT) viewing from F_o side to the F_1 side. Fig. 6B shows an example of the sequential clockwise rotation images with 100 ms interval. We have selected six rotational data points with different length filaments to show in Fig. 6C. The rotation displays occasional pause or even reversal due to Brownian fluctuation. The rotation speed decreases with the increasing length of filament , which is in agreement with the results of single molecule experiments of F_1[8,10] as expected.

Several control experiments were performed to confirm that the observed rotation is driven by transmembrane proton flow. As shown in Fig. 6D, the rotation stopped immediately once 5 μl of 10 μM CCCP was added. It was also found that if the sample is in the dark or is incubated with DCCD before illumination, no rotation was observed (data not shown) because CCCP destroyed the transmembrane p.m.f. as well as DCCD blocked the proton channels. Furthermore, if NaN_3 and ADP disappeared in the buffer, no rotation of filament was found because NaN_3 and ADP prevented the $\alpha_3\beta_3$ crown from sliding to the γ subunit.[69] These results demonstrated that the rotation of filaments depended on the p.m.f. produced in proteoliposome. It is interesting that the ΔpH transmembrane of proteoliposome can persist for a long time. After the illumination, some filaments rotated continuously for more than 20 min. Therefore, the proteoliposome functions as a recharge battery to supply energy to the rotary motor.

V. F_oF_1-ATPase activity regulated by external links on the stator

The activity regulation of the holoenzyme is an interesting topic. Traditional methods are chemical, which depend on either the

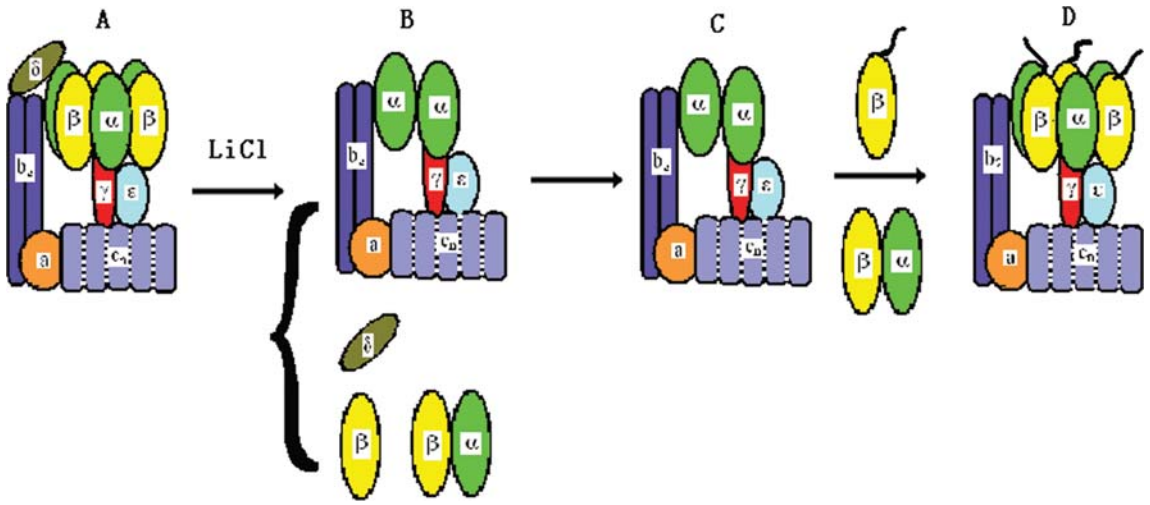

Fig. 5 The procedure for reconstituting δ-free F_oF_1-ATPase motor. (A) F_oF_1-ATPase; (B) F_oF_1-ATPase is treated by LiCl to remove δ subunit; (C) rebinding of purified β and α subunits; (D) the reconstituted δ-free F_oF_1-ATPase motor.[13]

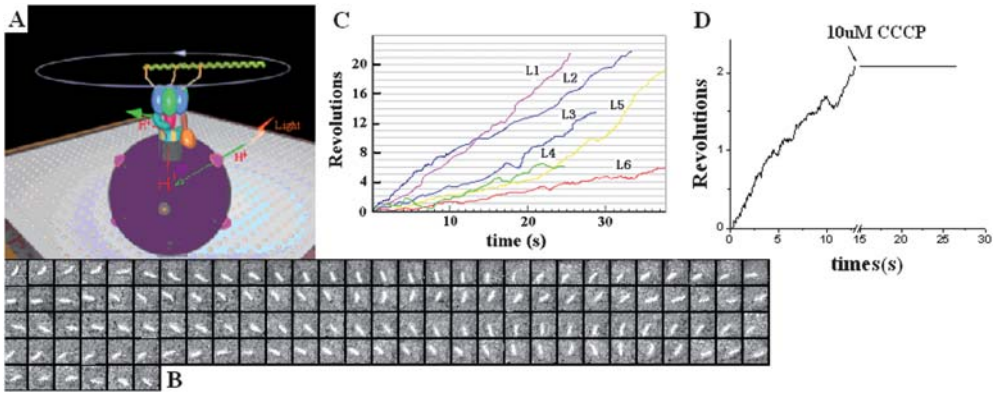

Fig. 6 (A) The system used for observation of the F_o in the proteoliposome which was immobilized on the cover glass with biotin–streptavidin–biotin. (B) The sequential images of a clockwise rotating fluorescent actin filament. Time interval is 100 ms. (C) Time courses of the actin filament rotation with different lengths. The fluorescent filament was attached to the β subunits through His-tag. The length of filaments denoted L1, L2, L3,L4 ,L5 and L6 are 1.7, 1.9, 2.0, 2.3, 2.8 and 3.3 μm respectively. (D) The rotation was inhibited by adding CCCP, which verified the motor was indeed driven by transmembrane ΔpH.[13]

concentration of substrate or the transmembrane electrochemical potential.[12,28,62,63] In fact, F_oF_1 motor actively converts a chemical reaction (ATP hydrolysis in F_1 or proton transfer in F_o) into unidirectional physical rotation of the "rotor", which is accompanied by the cyclic conformational change of the "stator". Single molecule assays have indicated that the activity of F_1[10,18] or the speed of F_o (δ free F_oF_1 motor)[13,20] can be regulated by varying the load on the "rotor" and the eccentric rotation of γ subunit is mechanically coupled with the cyclic conformational change of $\alpha_3\beta_3$ crown at a high efficiency. However, how to regulate the holoenzyme (including F_o and F_1) activity with a physical method instead a chemical one is still challenging. One of the reasons is that the "rotor" of F_oF_1 motor is mostly enwrapped by the "stator" $\alpha_3\beta_3$ crown. The other reason is that the exposed fraction of the "rotor" is also partly shaded by the b_2 subunit. Thus, it becomes very difficult to directly regulate the holoenzyme activity by a load on the "rotor".

Considering that the unidirectional rotation of "rotor" is tightly coupled with the cyclic conformational change of the "stator", what will happen to the activity of the rotary motor if external complexes bind to the "stator"? To study regulation of the F_oF_1-ATPase activity by a simple physical method, the influenza H9 virus and its special antibody were employed as external links on the β subunit. Firstly, the chromatophore was prepared from the cells of *Rhodopseudomonas palustris* according to ref. 70, in which F_o was embedded in the chromatophore,[71] whereas F_1 protruded outside (structure 0).[72] Next, the β antibody was bound to each β subunit (structure 1); then, streptavidin was connected to the β antibody (structure 2), and the H9 antibody was bound to the streptavidin in series *via* biotin (structure 3). Finally, the H9 virus was captured specifically by the H9 antibody (structure 4) (see Fig. 7). The holoenzyme activities of the five structures were measured by the luciferin–luciferase method with a computerized ultra-weak luminescence analyzer. All structures with different external links were treated as coordinates.[73–76]

The activity of native F_oF_1-ATPase was used as a control and other structures were compared with the native value. When the

Fig. 7 A schematic illustration of the activity regulation assay. The holoenzyme is a complex of two rotary motors F_o and F_1. F_o motor was constituted by a subunit (stator) and n channel (c_n, rotor). $\alpha_3\beta_3$ crown (stator) and γ subunit (rotor) formed the F_1 motor. The complex of b_2 and δ subunits fixed the two stators, whereas the two rotors are mechanically coupled by the ε subunit. External complexes are linked on β subunits to regulate the holoenzyme activity.

β antibody was bound, the F_oF_1-ATPase (structure 1) activities in both synthesis and hydrolysis decreased, and its relative value was about 85% of the native form (structure 0). If streptavidin was joined to the β antibody (structure 2), the enzyme synthesis/hydrolysis activities decreased to 87% of the activity of structure 1. After the H9 antibody was connected to streptavidin (structure 3), the enzyme activity was inhibited continuously, with a relative value of 75% of structure 2. Once H9 virus was captured by its antibody (structure 4), however, the motor was activated, and its relative synthesis and hydrolysis activities were about 210% of that of structure 3. It is amazing that the activity of the modified holoenzyme, in which a series of external complexes are linked on the stator, can exceed the native level. These results are indicated in Fig. 8.[77]

To identify whether the H9 virus directly affects F_oF_1-ATPase activity, we measured the activity of native buffer (structure 0) incubated with H9 virus. The results shown in Fig. 8 prove that the H9 virus doesn't have any direct effect on the holoenzyme

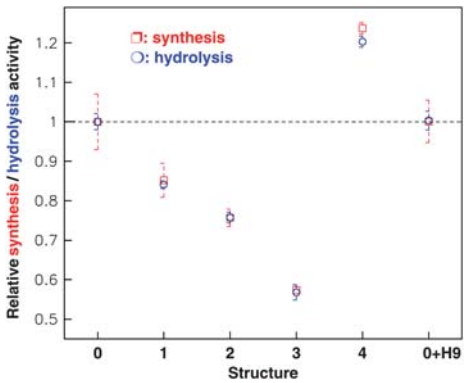

Fig. 8 Relative synthesis (red) and hydrolysis (green) activities of the holoenzyme with different links on the β subunit as shown in Fig. 7. The statistical value (mean s.e.m.) of each structure was computed from 50–60 samples. The experiment has been repeated independently more than five times (10 samples each time). The native F_oF_1-ATPase (structure 0) activity was taken as a control and others were expressed in proportion to the control. Structures 1, 2, 3 and 4 represent the F_oF_1-ATPase linking in series on the β antibody, streptavidin, H9 antibody and H9 virus respectively. 0 + H9 represents the holoenzyme mixed directly with the H9 virus.

activity no matter if the enzyme functions as a synthase or hydrolase.

The abnormal regulation from structure 3 to 4 implied that structure 3 has great potential in design of a rapid, unlabeled, sensitive and selective biosensor[78] though the underlying mechanism is still unclear.

VI. Conclusions

In contrast to human-made machines, motor proteins operate in a world where Brownian motion and viscous forces dominate. The relevant energy scale is k_BT, which amounts to 4 pN nm. This may be compared to the ~80 pN nm of energy derived from hydrolysis of a single ATP molecule at physiological conditions. Thermal, nondeterministic motion is thus an important aspect of the dynamics of molecular motors.

ATP hydrolysis does spontaneously occur in F_1, whereas the thermodynamically unfavorable reaction, ATP synthesis, has to be driven by harnessing the transmembrane proton flow in F_o. The mechanism of ATP formation in the F_1 part is well described by the "binding change mechanism". This has been developed in great detail by many techniques, and understanding of the mechanism has been claimed to be "almost complete". However, if the motor functions as a synthase, the two substrates, ADP and P_i, are recombined into one product, ATP. The binding order of the two substrates is still unclear. Another challenging question is whether the main kinetic enhancement occurs upon filling the second or the third site. For F_o, the torque generation between a and c_n in F_o is still covered. In addition, It has remained unsettled whether the entropic (chemical) component of $\Delta\tilde{\mu}_H^+$ relates to the difference in the proton activity between two bulk water phases (ΔpH^B) or between two membrane surfaces (ΔpH^S).[79]

It is of interest to ponder whether we can employ F_oF_1-ATPase nanomachines in artificial environments outside the cell to perform tasks that we design to our benefit.[80] One striking demonstration is the construction of a nickel nanopropeller that rotates through the action of an engineered F_1-ATPase motor.[81] A metal-binding site was engineered into the motor and acted as a reversible on–off switch by obstructing the rotation upon binding of a zinc ion,[82] similar to the action of putting a stick between two cogwheels. Other examples worth highlighting are the sol–gel packaging of vesicles containing bacteriorhodopsin, a light driven proton pump, and F_oF_1-ATP synthase,[83,84] or F_oF_1-ATPase embedded chromatophore.[76] Upon illumination, protons are pumped into the vesicles and ATP is created outside the vesicle by the ATP synthase. Besides the excellent stability of these gels (bacteriorhodopsin continued functioning for a few months), this technology provides a convenient packaging method and a way to use light energy for fuelling devices. Therefore, these nanodevices with a battery can be employed to design a rapid, unlabeled, sensitive and selective biosensor,[73–75,77] or construct a micro-mixer to accelerate thrombolysis.[67] Of course, many of these applications are little more than proof-of-principle examples.

Acknowledgements

This work was supported by the National Basic Research Program of China (973 Program) under the grant No. 2007CB935903 and No. 2007CB935901

References

1 P. D. Boyer, The ATP synthase—A splendid molecular machine, *Annu. Rev. Biochem.*, 1997, **66**, 717–749.
2 W. Junge, Protons, Proteins and ATP, *Photosynth. Res.*, 2004, **80**, 197–221.
3 J. Weber and A. E. Senior, ATP synthesis driven by proton transport in F_1F_o-ATP synthase, *FEBS Lett.*, 2003, **545**, 61–70.
4 C. von Ballmoos, A. Wiedenmann and P. Dimroth, Essentials for ATP synthesis by F_1F_o ATP synthase, *Annu. Rev. Biochem.*, 2009, **78**, 649–672.
5 B. A. Feniouk and M. Yoshida, Regulatory mechanisms of proton-translocating F_1F_o- ATP synthase, *Results Probl. Cell Differ.*, 2008, **45**, 279–308.
6 M. Saraste, Oxidative phosphorylation at the fin de siècle, *Science*, 1999, **283**, 1488–1493.
7 P. D. Boyer, R. L. Cross and W. Momsen, A new concept for energy coupling in oxidative phosphorylation based on a molecular explanation of the oxygen exchange reactions, *Proc. Natl. Acad. Sci. U. S. A.*, 1973, **70**, 2837–2839.
8 H. Noji, R. Yasuda, M. Yoshida and K. Kinosita Jr., Direct observation of the rotation of F_1-ATPase, *Nature*, 1997, **386**, 299–302.
9 J. P. Abrahams, A. G. W. Leslie, R. Lutter and J. E. Walker, Structure at 2.8 Å resolution of F_1-ATPase from bovine heart mitochondria, *Nature*, 1994, **370**, 621–628.
10 Y. Yasuda, H. Noji, K. Kinosita Jr. and M. Yoshida, F_1-ATPase is a highly efficient molecular motor that rotates with discrete 120° steps, *Cell*, 1998, **93**, 1117–1124.
11 T. Nishizaka and et.al, Chemomechanical coupling in F_1-ATPase revealed by simultaneous observation of nucleotide kinetics and rotation, *Nat. Struct. Mol. Biol.*, 2004, **11**, 142–148.
12 K. Adachi and et.al, Coupling of rotation and catalysis in F_1-ATPase revealed by single-molecule imaging and manipulation, *Cell*, 2007, **130**, 309–321.
13 Y. H. Zhang and et.al, Rotary torque produced by proton motive force in F_1F_o motor, *Biochem. Biophys. Res. Commun.*, 2005, **331**, 370–374.
14 M. G. Düser and et.al, 36° step size of proton-driven *c*-ring rotation in F_1F_o-ATP synthase, *EMBO J.*, 2009, **28**, 2689–2696.

15 G. Kaima and et.al, Coupled rotation within single F_1F_o enzyme complexes during ATP synthesis or hydrolysis, *FEBS Lett.*, 2002, **525**, 156–163.
16 M. Diez and et.al, Proton-powered subunit rotation in single membrane-bound F_1F_o-ATP synthase, *Nat. Struct. Mol. Biol.*, 2004, **11**, 135–141.
17 H. Ueno and et.al, ATP-driven stepwise rotation of F_oF_1-ATP synthase, *Proc. Natl. Acad. Sci. U. S. A.*, 2005, **102**, 1333–1338.
18 H. Itoh and et.al., Mechanically driven ATP synthesis by F_1-ATPase, *Nature*, 2004, **427**, 465–468.
19 Y. Rondelez and et.al, Highly coupled ATP synthesis by F_1-ATPase single molecules, *Nature*, 2005, **433**, 773–777.
20 X. L. Liu and et.al, Mechanically driven proton conduction in single δ-free F_oF_1-ATPase, *Biochem. Biophys. Res. Commun.*, 2006, **347**, 752–757.
21 Y. G. Shu and P. Y. Lai, Systematic kinetics study of F_1F_o-ATPase: Analytic results and comparison with experiments, *J. Phys. Chem. B*, 2008, **112**, 13453–13459.
22 J. Xing, J. C. Liao and G. Oster, Making ATP, *Proc. Natl. Acad. Sci. U. S. A.*, 2005, **102**, 16539–16546.
23 S. X. Sun, H. Wang and G. Oster, Asymmetry in the F_1-ATPase and its implications for the rotational cycle, *Biophys. J.*, 2004, **86**, 1373–1384.
24 H. Wang and G. Oster, Energy transduction in the F_1 motor of ATP synthase, *Nature*, 1998, **396**, 279–282.
25 T. Elston, H. Wang and G. Oster, Energy transduction in ATP synthase, *Nature*, 1998, **391**, 510–513.
26 G. Oster, H. Wang and M. Grabe, How F_o-ATPase generates rotary torque, *Philos. Trans. R. Soc. London, Ser. B*, 2000, **355**, 523–528.
27 A. Aksimentiev, I. A. Balabin, R. H. Fillingame and K. Schulten, Insights into the molecular mechanism of rotation in the F_o sector of ATP synthase, *Biophys. J.*, 2004, **86**, 1332–1344.
28 O. Pänke and B. Rumberg, Kinetic modelling of the proton translocating CF_oCF_1-ATP synthase from spinach, *FEBS Lett.*, 1996, **383**, 196–200.
29 O. Pänke and B. Rumberg, Kinetic modeling of rotary CF_oF_1-ATP synthase: storage of elastic energy during energy transduction, *Biochim. Biophys. Acta, Bioenerg.*, 1999, **1412**, 118–128.
30 B. R. Selman and S. Selman-Reiner, The steady state kinetics of photophosphorylation, *J. Biol. Chem.*, 1981, **256**, 1722–1726.
31 C. Kayalar, J. Rosing and P. D. Boyer, An alternating site sequence for oxidative phosphorylation suggested by measurement of substrate binding patterns and exchange reaction inhibitions, *J. Biol. Chem.*, 1977, **252**, 2486–2491.
32 J. A. Pérez and S. J. Ferguson, Kinetics of oxidative phosphorylation in *Paracoccus denitrificans*. 1. Mechanism of ATP synthesis at the active site(s) of F_oF_1-ATPase, *Biochemistry*, 1990, **29**, 10503–10518.
33 P. D. Boyer, Catalytic site forms and controls in ATP synthase catalysis, *Biochim. Biophys. Acta, Bioenerg.*, 2000, **1458**, 252–262.
34 Y. M. Milgrom and R. L. Cross, Rapid hydrolysis of ATP by mitochondrial F_1-ATPase correlates with the filling of the second of three catalytic sites, *Proc. Natl. Acad. Sci. U. S. A.*, 2005, **102**, 13831–13836.
35 A. E. Senior, S. Nadanaciva and J. Weber, The molecular mechanism of ATP synthesis by F_1F_o-ATP synthase, *Biochim. Biophys. Acta, Bioenerg.*, 2002, **1553**, 188–211.
36 C. Dou, P. A. G. Fortes and W. S. Allison, The $\alpha_3(\beta Y_{341}W)_3$ γ subcomplex of the F_1-ATPase from the thermophilic *bacillus* PS3 fails to dissociate ADP when MgATP is hydrolyzed at a single catalytic site and attains maximal velocity when three catalytic sites are saturated with MgATP, *Biochemistry*, 1998, **37**, 16757–16764.
37 R. I. Menz, J. E. Walker and A. G. W. Leslie, Structure of bovine mitochondrial F_1-ATPase with nucleotide bound to all three catalytic sites: implications for the mechanism of rotary catalysis, *Cell*, 2001, **106**, 331–341.
38 M. K. Al-Shawi, C. J. Ketchum and R. K. Nakamoto, The *Escherichia coli* F_oF_1 γM23K uncoupling mutant has a higher $K_{0.5}$ for P_i. transition state analysis of this mutant and others reveals that synthesis and hydrolysis utilize the same kinetic pathway, *Biochemistry*, 1997, **36**, 12961–12969.
39 J. A. Baylis Scanlon, M. K. Al-Shawi, N. P. Le and R. K. Nakamoto, Determination of the partial reactions of rotational catalysis in F_1-ATPase, *Biochemistry*, 2007, **46**, 8785–8797.
40 J. Weber and A. E. Senior, ATP synthase: what we know about ATP hydrolysis and what we do not know about ATP synthesis, *Biochim. Biophys. Acta, Bioenerg.*, 2000, **1458**, 300–309.
41 G. Kothen, O. Schwarz and H. Strotmann, The kinetics of photophosphorylation at clamped ΔpH indicate a random order of substrate binding, *Biochim. Biophys. Acta, Bioenerg.*, 1995, **1229**, 208–214.
42 J. Howard, *Mechanics of motor proteins and the cytoskeleton*, Sinauer Associates, Sunderland, MA (2001).
43 M. Schliwa, *Molecular motors*, Weinheim, Wiley-VCH, 2003.
44 F. Jülicher, A. Ajdari and J. Prost, Modeling molecular motors, *Rev. Mod. Phys.*, 1997, **69**, 1269–1281.
45 P. D. Boyer, The binding change mechanism for ATP synthase-Some probabilities and possibilities, *Biochim. Biophys. Acta, Bioenerg.*, 1993, **1140**, 215–250.
46 D. Stock, A. G. W. Leslie and J. E. Walker, Molecular architecture of the rotary motor in ATP synthase, *Science*, 1999, **286**, 1700–1705.
47 H. Seelert; et.al. Structural biology: Proton-powered turbine of a plant motor. 2000, 405, pp. 418–419.
48 W. P. Jiang, J. Hermolin and R. H. Fillingame, The preferred stoichiometry of c subunits in the rotary motor sector of *Escherichia coli* ATP synthase is 10, *Proc. Natl. Acad. Sci. U. S. A.*, 2001, **98**, 4966–4971.
49 N. Mitome, T. Suzuki, S. Hayashi and M. Yoshida, Thermophilic ATP synthase has a decamer c-ring: Indication of noninteger 10 : 3 H+/ATP ratio and permissive elastic coupling, *Proc. Natl. Acad. Sci. U. S. A.*, 2004, **101**, 12159–12164.
50 D. Pogoryelov and et.al, The c_{15} ring of the Spirulina platensis F-ATP synthase: F_1/F_o symmetry mismatch is not obligatory, *EMBO Rep.*, 2005, **6**, 1040–1044.
51 T. Meier and et.al, A tridecameric c ring of the adenosine triphosphate (ATP) synthase from the thermoalkaliphilic *Bacillus* sp. strain TA2.A1 facilitates ATP synthesis at low electrochemical proton potential, *Mol. Microbiol.*, 2007, **65**, 1181–1192.
52 P. Mitchell, Coupling of phosphorylation to electron and hydrogen transfer by a chemi-osmotic type of mechanism, *Nature*, 1961, **191**, 144–148.
53 U. Junesch and P. Gräber, Influence of the redox state and the activation of the chloroplast ATP synthase on proton-transport-coupled ATP synthesis/hydrolysis, *Biochim. Biophys. Acta, Bioenerg.*, 1987, **893**, 275–288.
54 U. Junesch and P. Gräber, The rate of ATP-synthesis as a function of ΔpH and $\Delta\Phi$ catalyzed by the active, reduced H^+-ATPase from chloroplasts, *FEBS Lett.*, 1991, **294**, 275–278.
55 P. Turina, Influence of the transmembrane electrochemical proton gradient on catalysis and regulation of the H^+-ATP synthase from, *Bioelectrochem. Bioenerg.*, 1994, **33**, 31–34.
56 D. Keller and C. Bustamante, The mechanochemistry of molecular motors, *Biophys. J.*, 2000, **78**, 541–556.
57 Y. G. Shu and H. L. Shi, Cooperative effects on the kinetics of ATP hydrolysis in collective molecular motors, *Phys. Rev. E: Stat., Nonlinear, Soft Matter Phys.*, 2004, **69**, 021912.
58 Y. G. Shu and H. L. Shi, The effect on mechanical tension on DNA polymerase activity studied with a two-state model, *Mod. Phys. Lett. B*, 2007, **21**, 1097–1105.
59 Y. G. Shu and Z. C. Ou-Yang, Motility of molecular motor, *J. Comput. Theor. Nanosci*, 2007, **4**, 71–76.
60 M. Li, Y. G. Shu and Z. C. Ou-Yang, Mechanochemical coupling of kinesin studied with a neck-linker swing model, *Commun. Theor. Phys.*, 2009, **51**, 1143–1148.
61 A. J. Hunt, F. Gittes and H. Howard, The force exerted by a single kinesin molecule against a viscous load, *Biophys. J.*, 1994, **67**, 766–781.
62 P. Turina, D. Samoray and P. Gräber, H^+/ATP ratio of proton transport-coupled ATP synthesis and hydrolysis catalysed by CF_oF_1-liposomes, *EMBO J.*, 2003, **22**, 418–426.
63 S. Steigmiller, P. Turina and P. Gräber, The thermodynamic H^+/ATP ratios of the H^+-ATPsynthases from chloroplasts and, *Proc. Natl. Acad. Sci. U. S. A.*, 2008, **105**, 3745–3750.
64 B. Böttcher and P. Gräber, Structural interpretations of F_o rotary function in the *Escherichia coli* F_1F_o ATP synthase, *Biochim. Biophys. Acta, Bioenerg.*, 2000, **1458**, 404–416.
65 Y. Moriyama, A. Iwamoto, H. Hanada, M. Maeda and M. Futai, One-step purification of *Escherichia coli* H^+-ATPase (F_1F_o) and its reconstitution into liposomes with neurotransmitter transporters, *J. Biol. Chem.*, 1991, **266**, 22141–22146.

66 T. Su and et.al, Constructing a novel Nanodevice powered by δ-free F_1F_o-ATPase, *Biochem. Biophys. Res. Commun.*, 2006, **350**, 1013–1018.
67 N. Tao, J. Cheng and J. C. Yue, Using F_1F_o-ATPase motors as micro-mixers accelerates thrombolysis, *Biochem. Biophys. Res. Commun.*, 2008, **377**, 191–194.
68 J. Y. Liao, J. Q. Yin and J. C. Yue, A novel biosensor to detect microRNAs rapidly, *Journal of Sensors*, 2009, DOI: 10.1155/671896.
69 E. Muneyuki and et.al, Inhibitory effect of NaN_3 on the F_oF_1 ATPase of submitochondrial particles as related to nucleotide binding, *Biochim. Biophys. Acta, Bioenerg.*, 1993, **1144**, 62–68.
70 S. Philosoph, A. Binder and Z. Gromet-Elhanan, Coupling factor ATPase complex of Rhodospirillum rubrum. Purification and properties of a reconstitutively active single subunit, *J. Biol. Chem.*, 1977, **252**, 8747–8752.
71 B. A. Feniouk and et.al, Chromatophore vesicles of *Rhodobacter capsulatus* contain on average one F_oF_1-ATP synthase each, *Biophys. J.*, 2002, **82**, 1115–1122.
72 T. Geyer and V. Helms, A spatial model of the chromatophore vesicles of *Rhodobacter sphaeroides* and the position of the cytochrome bc_1 complex, *Biophys. J.*, 2006, **91**, 921–926.
73 X. L. Liu and et.al, F_oF_1-ATPase as biosensor to detect single virus, *Biochem. Biophys. Res. Commun.*, 2006, **342**, 1319–1322.
74 Z. T. Deng and et.al., Green and orange CdTe quantum dots as effective pH-sensitive fluorescent probes for dual simultaneous and independent detection of viruses, *J. Phys. Chem. B*, 2007, **111**, 12024–12031.
75 Y. Zhang and et.al, Using cadmium telluride quantum dots as a proton flux sensor and applying to detect H9 avian influenza virus, *Anal. Biochem.*, 2007, **364**, 122–127.
76 Y. B. Cui, Z. Fan and J. C. Yue, Detecting proton flux across chromatophores driven by F_oF_1-ATPase using *N*-(fluorescein-5-thiocarbamoyl)-1,2-dihexadecanoyl- *sn*-glycero- 3-phosphoethanolamine, triethylammonium salt, *Anal. Biochem.*, 2005, **344**, 102–107.
77 J. Cheng, X. A. Zhang, Y. G. Shu and J. C. Yue, F_oF_1-ATPase activity regulated by external links on β subunits, *Biochem. Biophys. Res. Commun.*, 2010, **391**, 182–186.
78 J. York, D. Spetzler, F. S. Xiong and W. D. Frasch, Single-molecule detection of DNA *via* sequence-specific links between F_1-ATPase motors and gold nanorod sensors, *Lab Chip*, 2008, **8**, 415–419.
79 D. A. Cherepanov, B. A. Feniouk, W. Junge and A. Y. Mulkidjanian, Low dielectric permittivity of water at the membrane interface: effect on the energy coupling mechanism in biological membranes, *Biophys. J.*, 2003, **85**, 1307–1316.
80 M. G. L. van den Heuvel and C. Dekker, Motor proteins at work for nanotechnology, *Science*, 2007, **317**, 333–336.
81 R. K. Soong, G. D. Bachand, H. P. Neves, A. G. Olkhovets, H. G. Craighead and C. D. Montemagno, Powering an inorganic nanodevice with a biomolecular motor, *Science*, 2000, **290**, 1555–1558.
82 H. Liu, J. J. Schmidt, G. D. Bachand, S. S. Rizk, L. L. Looger, H. W. Hellinga and C. D. Montemagno, Control of a biomolecular motorpowered nanodevice with an engineered chemical switch, *Nat. Mater.*, 2002, **1**, 173–177.
83 T.-J. M. Luo, R. Soong, E. Lan, B. Dunn and C. Montemagno, Photo-induced proton gradients and ATP biosynthesis produced by vesicles encapsulated in a silica matrix, *Nat. Mater.*, 2005, **4**, 220–224.
84 H. J. Choi and C. D. Montemagno, Artificial Organelle: ATP Synthesis from cellular mimetic polymersomes, *Nano. Lett.*, 2005, **5**, 1538–1542.